

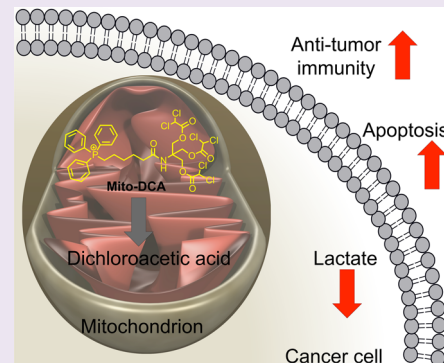
Mito-DCA: A Mitochondria Targeted Molecular Scaffold for Efficacious Delivery of Metabolic Modulator Dichloroacetate

Rakesh K. Pathak,^{†,§} Sean Marrache,^{†,§} Donald A. Harn,[‡] and Shanta Dhar^{*,†}

[†]NanoTherapeutics Research Laboratory, Department of Chemistry and [‡]Department of Infectious Diseases, University of Georgia, Athens, Georgia 30602, United States

 Supporting Information

ABSTRACT: Tumor growth is fueled by the use of glycolysis, which normal cells use only in the scarcity of oxygen. Glycolysis makes tumor cells resistant to normal death processes. Targeting this unique tumor metabolism can provide an alternative strategy to selectively destroy the tumor, leaving normal tissue unharmed. The orphan drug dichloroacetate (DCA) is a mitochondrial kinase inhibitor that has the ability to show such characteristics. However, its molecular form shows poor uptake and bioavailability and limited ability to reach its target mitochondria. Here, we describe a targeted molecular scaffold for construction of a multiple DCA loaded compound, Mito-DCA, with three orders of magnitude enhanced potency and cancer cell specificity compared to DCA. Incorporation of a lipophilic triphenylphosphonium cation through a biodegradable linker in Mito-DCA allowed for mitochondria targeting. Mito-DCA did not show any significant metabolic effects toward normal cells but tumor cells with dysfunctional mitochondria were affected by Mito-DCA, which caused a switch from glycolysis to glucose oxidation and subsequent cell death *via* apoptosis. Effective delivery of DCA to the mitochondria resulted in significant reduction in lactate levels and played important roles in modulating dendritic cell (DC) phenotype evidenced by secretion of interleukin-12 from DCs upon activation with tumor antigens from Mito-DCA treated cancer cells. Targeting mitochondrial metabolic inhibitors to the mitochondria could lead to induction of an efficient antitumor immune response, thus introducing the concept of combining glycolysis inhibition with immune system to destroy tumor.



Stimulation of mitochondrial activity and alterations of cancer cell characteristic adenosine-5'-triphosphate (ATP) generation pathways can be an efficient method in anticancer therapeutic strategy.^{1–6} The small molecule mitochondrial kinase inhibitor dichloroacetate (DCA) has the potential to become a major player in the field of cancer chemotherapy.^{7–10} By utilizing the metabolic switch, DCA reverses cancer cell abnormal metabolism from aerobic glycolysis to glucose oxidation by reducing the activity of mitochondrial pyruvate dehydrogenase kinase 1 (PDK1),¹¹ which negatively regulates pyruvate dehydrogenase (PDH) causing pyruvate to convert to acetyl-CoA, promoting oxidative phosphorylation (OX-PHOS).⁷ DCA reduces high mitochondrial membrane potential ($\Delta\psi_m$) and increases mitochondrial reactive oxygen species (ROS) in malignant but not in normal cells.⁷

Therapeutically prohibitive high DCA doses are needed for tumor growth suppression due to the lack of effective cellular uptake¹² and its localization inside the target organelle, the mitochondria of cells. There are limited efforts for direct use of DCA in cancer patients due to the fact that finding funding for clinical trials is a challenge since DCA is a generic drug for lactic acidosis.¹⁰ In physiological conditions, orally or intravenously administered DCA is ionized and cannot pass through the plasma membrane by passive diffusion. We raised two questions: how to introduce physiologically relevant DCA doses into cancer cells and how to engineer the anionic form of

DCA to partition across the inner mitochondrial membrane (IMM) and the negative $\Delta\psi_m$ that exists across this membrane into the matrix to access PDK1? Like other mitochondria acting therapeutics, DCA encounters tremendous barriers in its navigation to enter the mitochondria. Since the monocarboxylate transporters that are linked to DCA cellular entry are electroneutral in most cells including tumor,¹³ we questioned the ability of these transporters to accumulate anionic DCA in tumor. Moreover, for mitochondrial uptake, DCA competes with pyruvate for its entry *via* the mitochondrial pyruvate transporter. Recent studies identified that sodium-coupled monocarboxylate transporter or solute carrier family-5 member-8 would accept DCA as a substrate.^{14,15} However, this transporter is expressed in normal cells, but expression is silenced in tumor cells.^{16,17} Lactate is the most abundant product of highly glycolytic tumors and high levels of extracellular lactate cause blocking of monocyte differentiation to dendritic cells (DCs), significant inhibition of cytokine release from DCs and cytotoxic T lymphocytes, inhibition of monocyte migration, and reduction of cytotoxic T-cell function.¹⁸ Inhibition of cancer cell glycolysis using DCA has

Received: December 26, 2013

Accepted: March 11, 2014

Published: March 11, 2014

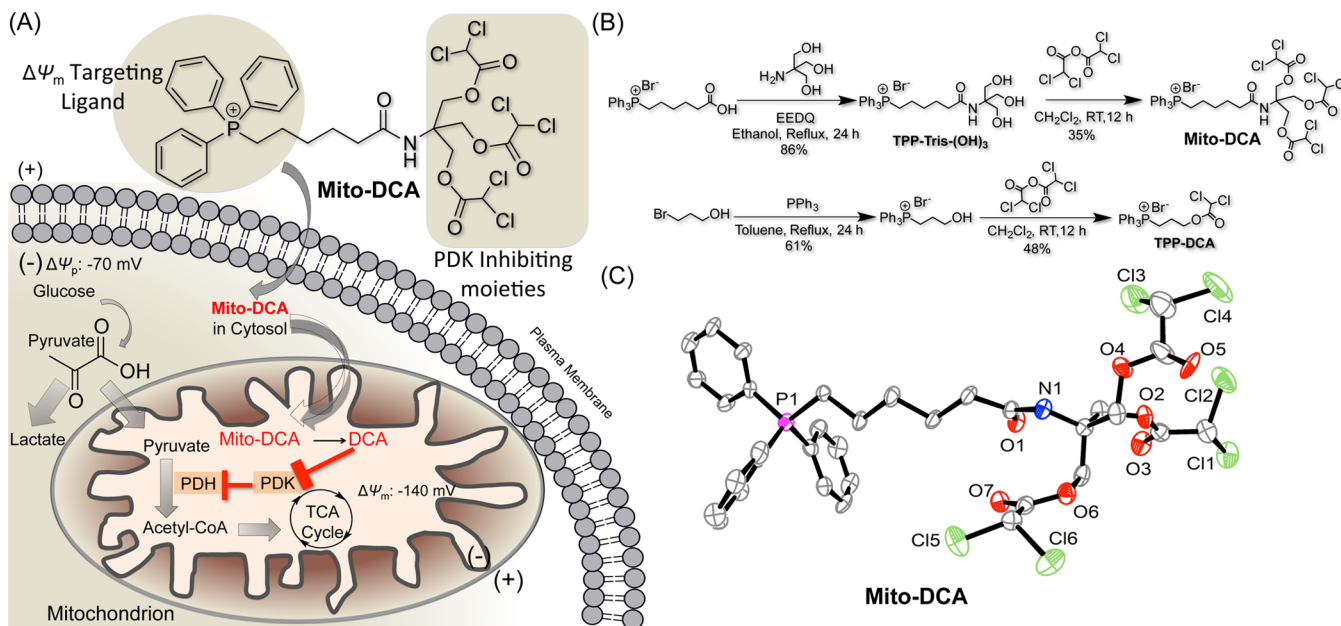


Figure 1. (A) Design of Mito-DCA and its possible mechanism of action. (B) Synthesis of mitochondria-targeted DCA analogues. (C) ORTEP diagram of Mito-DCA with 50% thermal ellipsoids.

the potential to overcome the immune suppressive nature of a glycolytic tumor; however, it needs very high DCA doses. We hypothesized that DCA needs to be engineered for efficient cellular and mitochondrial uptake to show efficient glycolytic inhibition, to exhibit anticancer activity, and to enhance the effects of antitumor immunity at pharmacologically relevant doses.

Taking advantage of the higher $\Delta\psi_m$ of cancer cells, we investigated a means to circumvent the low efficacy of DCA by targeted delivery using a lipophilic triphenylphosphonium (TPP) cation, which equilibrates across the membranes in a Nernstian fashion and accumulates into the mitochondrial matrix (Figure 1).^{19–24} Here, we report a technology for construction of a mitochondria targeted DCA analogue, Mito-DCA, by incorporating a TPP moiety and its ability to selectively alter cancer cell metabolism (Figure 1A).

RESULTS AND DISCUSSION

Design and Construction of Mito-DCA. Major challenges in designing chemistries to incorporate drug molecules and targeting moieties include compatibility of the carrier and the drug, carrier induced immunogenic responses, unbalanced increase in lipophilicity, stability and activity of the drug, and the number of available attachment sites for drug conjugation. With such issues in mind, we designed Mito-DCA (Figure 1A). DCA mediated inactivation of PDK1 kinase activity requires DCA to be bound with the N-terminal helix bundle of PDK.²⁵ Such a binding causes local conformational changes in PDK1, which communicate to both nucleotide and lipoyl-binding pockets, leading to inhibition of kinase activity. In Mito-DCA, the mitochondria targeting TPP cation was introduced *via* a comparatively stable amide linkage, and multiple DCA molecules were incorporated *via* tris(hydroxymethyl)-aminomethane (Tris)²⁶ using esterase-labile ester bonds. We hypothesized that this design would allow release of DCA molecules in an esterase-dependent manner under physiological conditions for effective PDK1 binding without having any steric encumbrance from the bulky TPP moiety. The use of

comparatively stable amide linkage for TPP conjugation will allow Mito-DCA to navigate into the mitochondria (Figure 1A). The difference between plasma membrane potential and $\Delta\psi_m$ will allow Mito-DCA to be concentrated within mitochondria with respect to the cytosol at a much faster rate before it can undergo any premature hydrolysis by the esterases present in the cytosol.²⁷ To construct Mito-DCA, TPP-Tris-(OH)₃ was synthesized by reacting (S-carboxypentyl)triphenylphosphonium bromide (Figures S1 and S2 in the Supporting Information) with Tris in the presence of *N*-ethoxycarbonyl-2-ethoxy-1,2-dihydroquinoline (EEDQ), a highly specific reagent that enables coupling of an amine with a carboxyl group in the presence of a hydroxyl functionality (Figure 1B, Figures S3 and S4 in the Supporting Information). The hydroxyl groups from TPP-Tris-(OH)₃ were coupled with DCA-anhydride to give Mito-DCA. Formation of Mito-DCA was confirmed by spectroscopic and analytical methods (Figures S5, S6 in the Supporting Information). The structure was confirmed by X-ray crystallographic analysis (Figure 1C). Details of the structure are available in Tables S1 and S2 and Figure S7 in the Supporting Information. A chromatographic analysis on Mito-DCA showed a single peak, confirming the purity (Figure S8 in the Supporting Information). These characterizations indicated that Mito-DCA has the proposed structure (Figure 1). Low concentration of delocalized lipophilic TPP cation is sufficient for localization to the mitochondria, but at elevated concentrations, such a cation induces mitochondrial membrane disruption.²⁸ The present design strategy allowed for loading of three DCA molecules per TPP in Mito-DCA, enabling us to deliver higher DCA dose using low TPP concentration to avoid such disruption. To probe that delivering multiple DCA molecules using a single TPP moiety can be beneficial, we synthesized TPP-DCA with one DCA per TPP (Figure 1B, Figures S11 and S12 in the Supporting Information). Solubility of Mito-DCA in water was checked by preparing different concentrations of Mito-DCA ranging from 2 μ M to 5 mM in 0.1–2.5% dimethylsulfoxide (DMSO)-phosphate buffered saline (PBS)

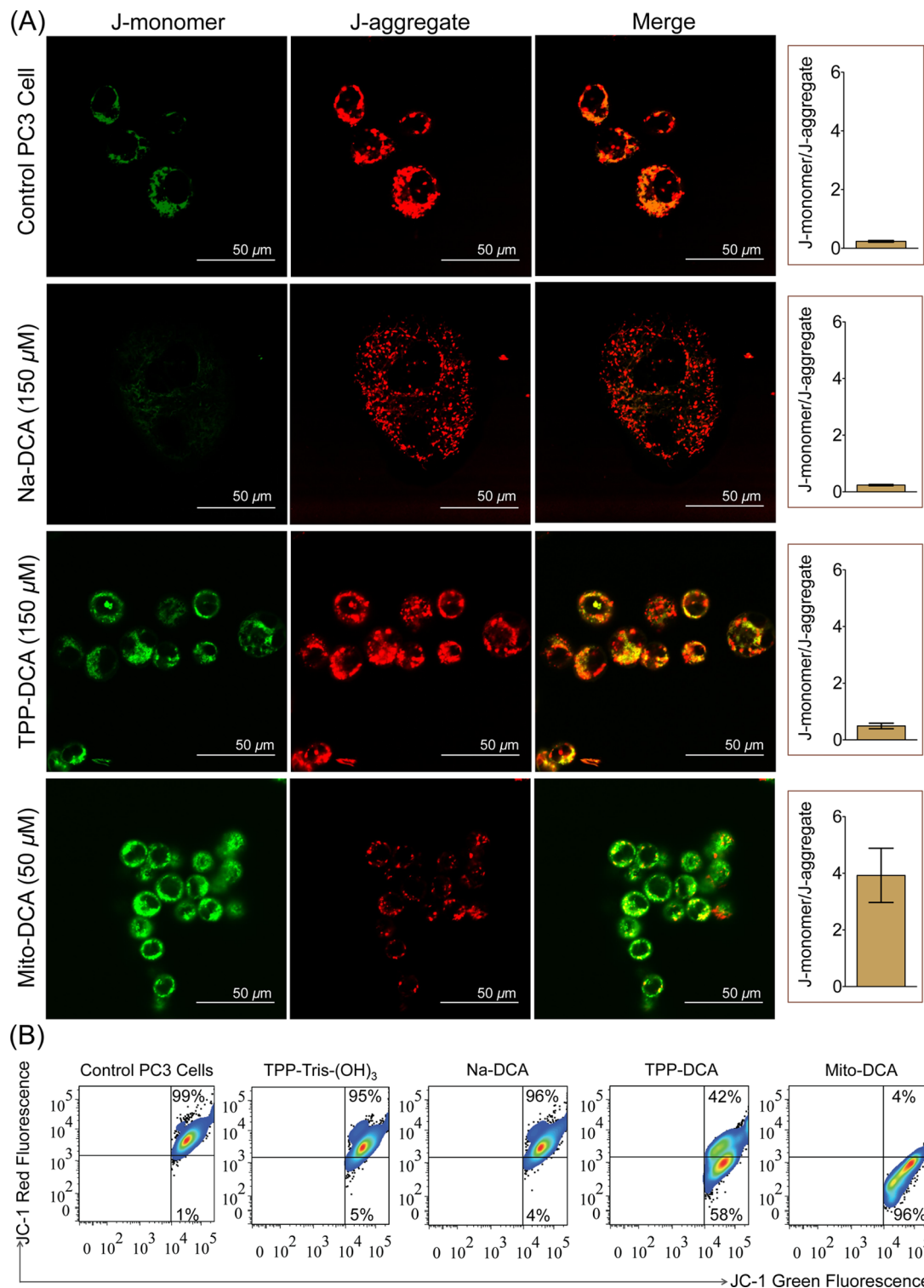


Figure 2. Changes in the $\Delta\psi_m$ by JC-1 assay. Treatment of PC3 cells with Mito-DCA dramatically caused the collapse of $\Delta\psi_m$ in these cells compared to Na-DCA or TPP-DCA. Cells were stained with JC-1. Green fluorescence, depolarized mitochondria (J-monomer); red fluorescence, hyperpolarized (J-aggregates). (A) The shift in $\Delta\psi_m$ observed by disappearance of red-orange-stained mitochondria (large negative $\Delta\psi_m$) and an increase in fluorescent green-stained mitochondria (loss of $\Delta\psi_m$) by Mito-DCA is higher compared to that observed by TPP-DCA or Na-DCA as determined by confocal microscopy. The JC-1 green/red ratio results from the mitochondria in all four groups are shown at the right. (B) PC3 cells treated under the same conditions as mentioned above were analyzed on a flow cytometer.

(Figure S13 in the Supporting Information). At all concentrations, solutions were transparent and no precipitation was observed. Solubility of Mito-DCA was far higher than that of DCA in an organic solvent, showing its lipophilicity for

mitochondrial uptake. It is essential that Mito-DCA releases active DCA under physiological conditions so as to obtain maximum PDK1 binding, and substituents left on DCA could significantly lower its PDK1 binding due to steric hindrance.

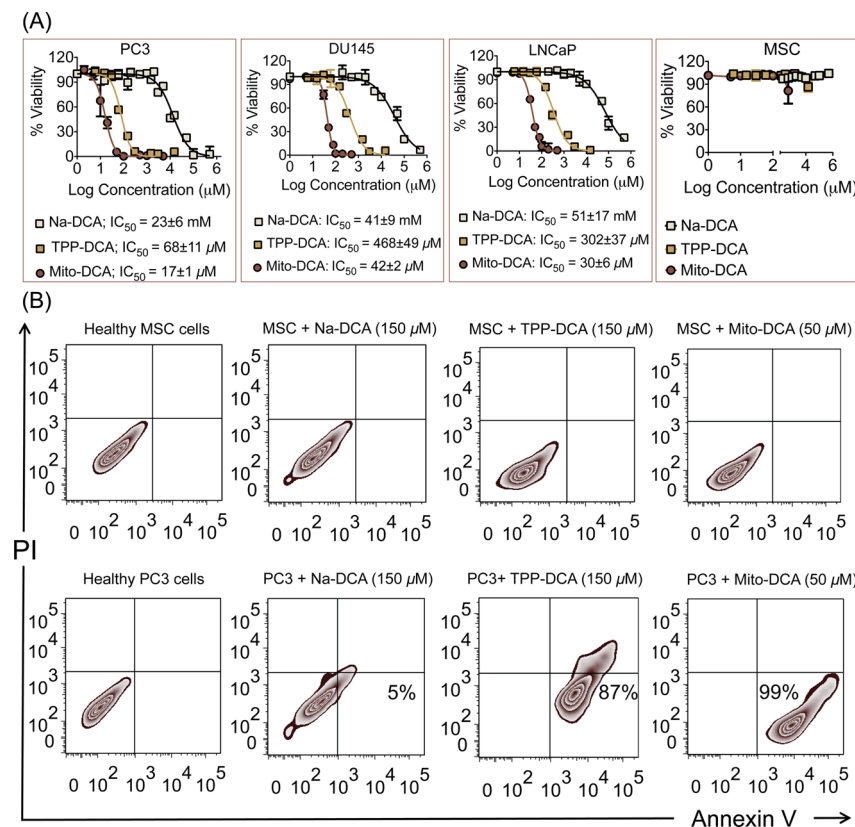


Figure 3. (A) Highly glycolytic PC3 and DU145 cells respond differently to Mito-DCA compared to less glycolytic LNCaP cells; Mito-DCA, TPP-DCA, and Na-DCA have no toxicity in MSC cells. Cells on 96-well plates were treated with varied concentrations of Mito-DCA, TPP-DCA, and Na-DCA for 72 h and viability was assessed by the MTT assay. A representative experimental data are shown in the figure and the IC₅₀ values were calculated from three independent experiments. (B) FACS analysis using Annexin V-Alexa Fluor/PI staining for apoptosis detection in MSC and PC3 cells on treatment with Mito-DCA, TPP-DCA, and Na-DCA for 12 h. Cells in the lower right quadrant indicate Annexin V-positive/PI negative, early apoptotic cells. The cells in the upper right quadrant indicate Annexin V-positive/PI positive, late apoptotic or necrotic cells.

Mito-DCA was incubated in PBS solution (pH 7.4) in order to check the release of DCA. The ester bonds in Mito-DCA were cleaved sequentially to release all three DCA molecules without disrupting the amide linkage (Figure S14 in the Supporting Information).

Mitochondrial Membrane Potential and Mito-DCA.

We next investigated the effect of Mito-DCA on cancer cell Δψ_m using a cationic dye, 5,5',6,6'-tetrachloro-1,1',3,3'-tetraethylbenzimidazolylcarbocyanine iodide or JC-1, that exhibits potential-dependent accumulation in the mitochondria accompanied by a fluorescence emission shift from green to red due to the concentration-dependent formation of red fluorescent 'J-aggregates'. Mitochondrial depolarization is indicated by an increase in the green/red fluorescence intensity ratio. Live cell imaging of PC3 cells treated with Na-DCA (150 μM), TPP-DCA (150 μM), or Mito-DCA (50 μM) for 6 h at 37 °C, followed by staining with JC-1, and a comparative analysis of JC-1 green/red fluorescence ratio in response to these three DCA analogues are represented in Figure 2A. Quantitative analysis of JC-1-stained PC3 cells revealed a significant decrease in the red (high Δψ_m) to green (low Δψ_m) ratio in Mito-DCA (green:red, 3.96 ± 0.96) treated cells compared with control cells (green:red, 0.24 ± 0.03) or the cells that were treated with Na-DCA (green:red, 0.24 ± 0.02) at an equivalent DCA concentration. TPP-DCA showed a green:red ratio of 0.49 ± 0.09, which was significantly lower than the ratio given by Mito-DCA. Treatment of PC3 cells with TPP-Tris-(OH)₃ (50 μM) for 6 h at 37 °C did not show any

changes in Δψ_m (Figure S15 in the Supporting Information). As a positive control of Δψ_m collapse, carbonyl cyanide 4-(trifluoromethoxy)phenylhydrazone (FCCP) was used, which indicated mitochondrial depolarization in PC3 cells compared to untreated control cells (Figure S15 in the Supporting Information). As mentioned above, depending on the Δψ_m, JC-1 accumulates selectively within intact mitochondria to form J-aggregates emitting fluorescence light at 585 nm, and the J-monomer emits at 530 nm upon excitation with 488 nm light. Thus, we also carried out a quantitative analysis of mitochondrial functions of cells treated with Mito-DCA, TPP-DCA, Na-DCA, and TPP-Tris-(OH)₃ under the same set of conditions as mentioned above in the presence of JC-1 using fluorescence activated cell sorting (FACS) with green fluorescence in channel 1 (FL1) and orange emission in channel 2 (FL2) (Figure 2B). Mito-DCA treatment of PC3 cells resulted in increase in the numbers of green-fluorescence-positive cells as shown in the lower right quadrant of the FACS histogram (96%). Under the same conditions, TPP-Tris-(OH)₃ or Na-DCA did not show green-fluorescence-positive populations. The number of green-fluorescence-positive cells (58%) in TPP-DCA was fewer compared to Mito-DCA. Collectively, these studies indicated the ability of Mito-DCA to cause reduction in Δψ_m in a highly glycolytic PC3 cells at a low concentration of 50 μM due to the incorporation of mitochondria targeting moiety and loading of multiple DCA units in a single molecule. We investigated whether DCA released from Mito-DCA can restore the hyperpolarization of

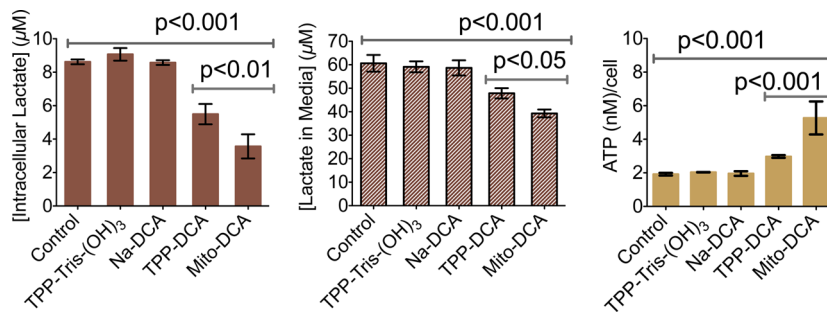


Figure 4. Lactate levels in PC3 cells (left) and media (middle) after treatment with 150 μM Na-DCA, 150 μM TPP-DCA, and 50 μM Mito-DCA for 6 h at 37 °C. Changes in intracellular ATP content (right) associated with the lactate fluctuation in the PC3 cells after treatment with 60 μM Na-DCA, 60 μM TPP-DCA, and 20 μM Mito-DCA for 3 h at 37 °C.

PC3 cells by carrying out a tetramethyl rhodamine methyl ester (TMRM) assay. In general, cancer cells have significantly more hyperpolarized $\Delta\psi_m$ and therefore control PC3 cells exhibited increased fluorescence of the $\Delta\psi_m$ -sensitive positive TMRM. Treatment of PC3 cells with Mito-DCA for 6 h reversed the hyperpolarization; in contrast, Na-DCA, TPP-DCA, and TPP-Tris-(OH)₃ did not alter the $\Delta\psi_m$ of the PC3 cells (Figure S16 in the Supporting Information).

Mito-DCA is More Effective in Highly Glycolytic Cancer Cells. Amplified glucose consumption and energy production from glycolysis are basic characteristics of most malignant cells; however, prostate cancer (PCa) cells have unique metabolic characteristics. Glycolytic profiles in androgen-dependent and androgen-independent PCa stages are not well understood.²⁹ The metabolic switching ability of Mito-DCA was studied on different PCa cell types. We used androgen-responsive LNCaP and androgen-nonresponsive PC3 and DU145 PCa cells. LNCaP cells have a significantly greater oxygen consumption and lower rate of lactate production compared to PC3 cells.³⁰ Mesenchymal precursor cells are believed to be the origin for various types of sarcoma, and the transformation of these stem cells is a prerequisite for the development of most human malignancies.³¹ We therefore used human mesenchymal stem cells (MSCs) as controls to examine the toxicity profile of Mito-DCA on normal cells. Representative cell viability profiles for PC3, DU145, LNCaP, and MSC cells after treatment with various concentrations of Mito-DCA, TPP-DCA, and Na-DCA for 72 h are shown in Figure 3A. The cytotoxicity profiles of TPP-Tris-(OH)₃, the carrier for targeted delivery of DCA to the mitochondria of cells shown in Figure S17 in the Supporting Information, demonstrated nontoxic behavior of the carrier in PCa and MSC cells even at millimolar concentrations. Results indicated that Na-DCA is less active in all three PCa cell lines irrespective of their glycolytic states with IC₅₀ values in the range of 20–40 mM in highly glycolytic PC3 and DU145 cells to >50 mM in less glycolytic LNCaP cells [IC₅₀(PC3): 23 ± 6 mM; IC₅₀(DU145): 41 ± 9 mM; IC₅₀(LNCaP): 51 ± 17 mM], and no toxicity was observed in MSC cells. In contrast, when multiple DCA molecules were delivered directly to the mitochondria using a single TPP moiety in the form of Mito-DCA, a remarkable increase in cytotoxicity in all three PCa cell lines was observed. Mito-DCA with an IC₅₀ value of 17 ± 1 μM in highly glycolytic PC3 cells was found to be 3 orders of magnitude more active compared to Na-DCA. Similar trends were observed in DU145 (IC₅₀: 42 ± 2 μM) and LNCaP (IC₅₀: 30 ± 6 μM) cells; Mito-DCA showed 3 orders of magnitude more activity than Na-DCA. TPP-DCA [IC₅₀(PC3): 68 ± 11 μM; IC₅₀(DU145): 468 ± 49

μM; IC₅₀(LNCaP): 302 ± 37 μM] in PC3 cells was ~4 times and in LNCaP and DU145 cells ~10 times less active than Mito-DCA. In MSCs, both Mito-DCA and TPP-DCA did not show any toxic effects at these concentrations, demonstrating their unique cancer cell selectivity.

In order to determine whether the enhanced activity of Mito-DCA was due to apoptosis or necrosis, we carried out an Alexa Fluor 488-Annexin-V-propidium iodide (PI) cell staining in PC3 and MSC cells and analyzed the results using FACS (Figure 3B). As controls, etoposide treated cells were used as early apoptosis population and H₂O₂ treated cells were marked as late apoptotic or necrotic population (Figure S18 in the Supporting Information). MSC cells did not undergo apoptosis with Mito-DCA (50 μM), TPP-DCA (150 μM), and Na-DCA (150 μM) treatment for 12 h at 37 °C. However, at a low concentration of Mito-DCA (50 μM), complete early apoptosis was observed in PC3 cells; TPP-DCA showed similar behavior at 150 μM, and no apoptosis was detected with Na-DCA at a concentration of 150 μM. There were no late apoptotic or necrotic populations observed with these compounds.

Selective Alteration of Cancer Cell Glucose Metabolism by Mito-DCA. Cytosolic metabolism of glucose to pyruvate occurs before its entry into the mitochondria for OXPHOS. Glycolysis in the absence of OXPHOS in cancer causes an increase in lactate. To test the ability of Mito-DCA to inhibit glycolysis in cancer cells, we measured intracellular lactate levels in glycolytic PC3 cells and in the media and compared these values with those observed in less glycolytic LNCaP cells and normal MSCs (Figure 4, Figure S19 in the Supporting Information). Mito-DCA decreased extracellular and intracellular lactate levels of PC3 cells in a dose-dependent manner (Figure 4, Figure S19 in the Supporting Information). A low Mito-DCA concentration of 10 μM and an incubation period of 3 h inhibited the extra- and intracellular lactate levels marginally (Figure S19A in the Supporting Information). Intracellular lactate ($P < 0.0112$) and extracellular lactate ($P < 0.0076$) levels of PC3 cells were significantly decreased at this concentration of Mito-DCA compared with the control cells. In contrast, TPP-DCA and Na-DCA at a low concentration of 30 μM and an incubation period of 3 h did not exhibit any changes in the intracellular and extracellular lactate levels (Figure S19A in the Supporting Information). The targeted carrier TPP-Tris-(OH)₃ under these conditions did not alter the lactate levels in the treated PC3 cells (Figure S19A in the Supporting Information). Treatment of PC3 cells with 50 μM Mito-DCA for 6 h showed significant reduction in lactate levels both in the cells and in the media (Figure 4). Cells treated with the control delivery scaffold TPP-Tris-(OH)₃ did not show any effect. PC3

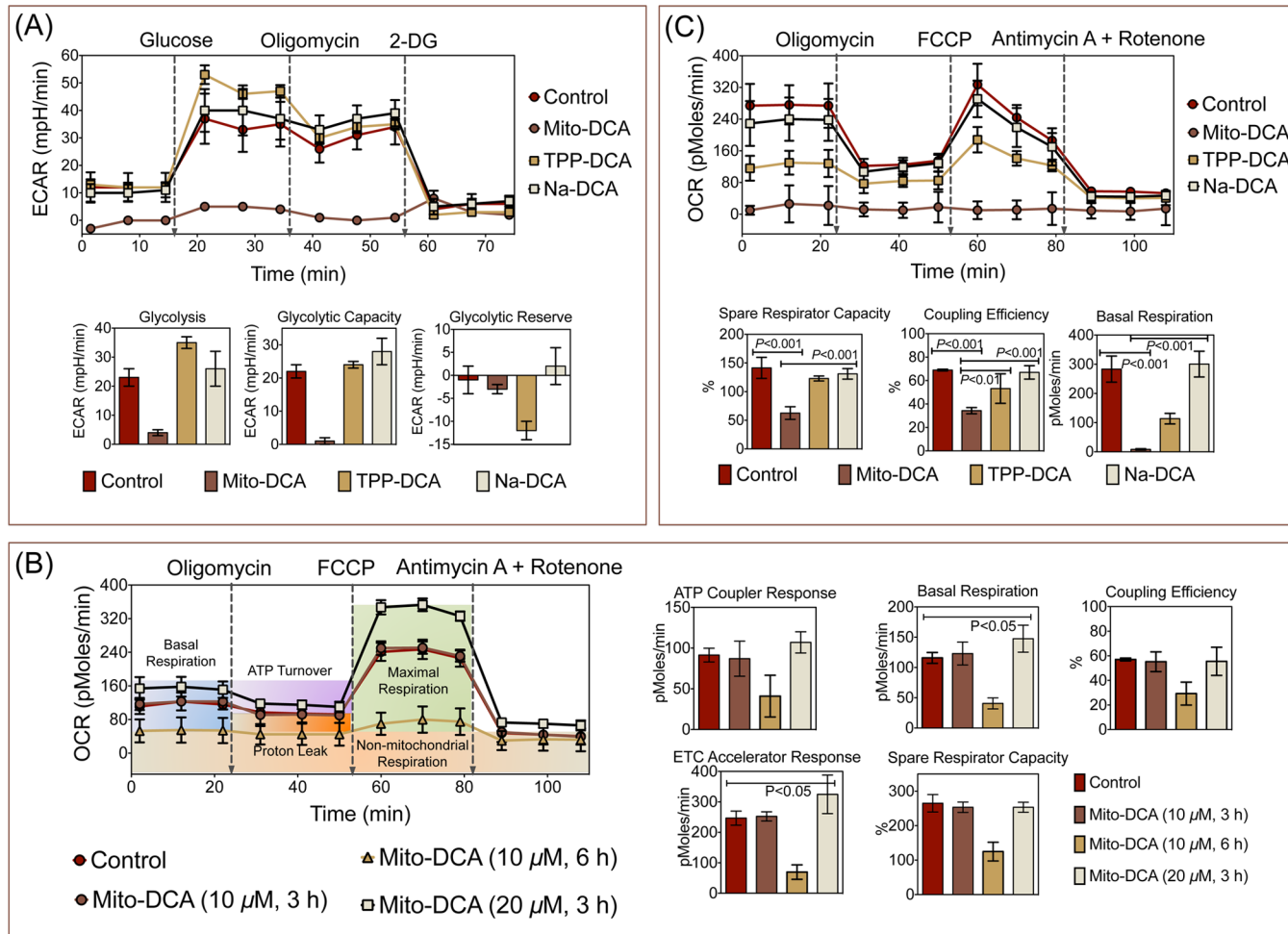


Figure 5. (A) Effect of Mito-DCA, TPP-DCA, and Na-DCA on PC3 cell glycolysis. PC3 cells were treated with 10 μ M Mito-DCA, 30 μ M TPP-DCA, or 30 μ M Na-DCA for 4 h. ECAR following the addition of glucose represents glycolysis, ECAR following oligomycin shows maximum glycolytic capacity, and ECAR following treatment with 2-DG represents acidification associated with nonglycolytic activity. PC3 cells were subsequently treated with glucose, oligomycin, and 2-DG. (B) Effect of Mito-DCA on OCR of PC3 cells. PC3 cells were treated with 10 μ M Mito-DCA for 3 h, 10 μ M Mito-DCA for 6 h, or 20 μ M Mito-DCA for 3 h. OCR traces were determined using a Seahorse mito stress kit and Seahorse XF24 analyzer. OCR prior to the addition of oligomycin and following the treatment of FCCP represent the basal mitochondrial respiration and maximal mitochondrial respiration capacity, respectively. OCR following rotenone plus antimycin A treatment represents non-mitochondrial respiration. (C) A comparison of the effects of Mito-DCA, TPP-DCA, and Na-DCA on OCR of PC3 cells. PC3 cells were treated with 10 μ M Mito-DCA, 30 μ M TPP-DCA, or 30 μ M Na-DCA for 4 h.

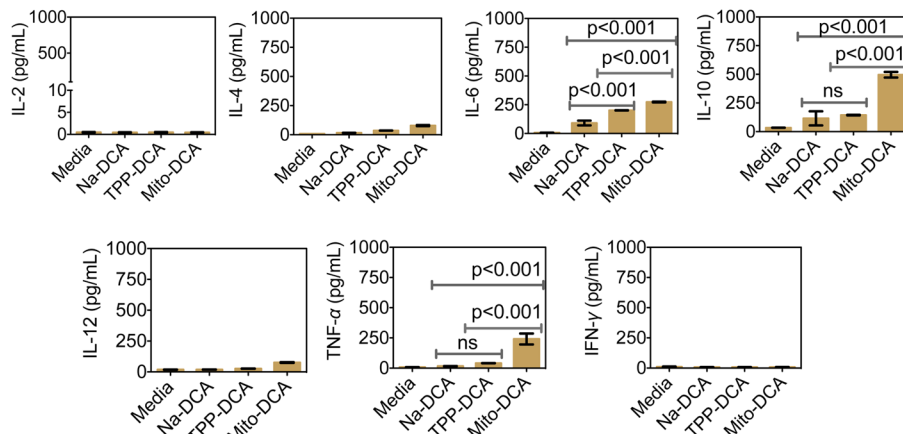
cells treated with 150 μ M of Na-DCA showed no effect. TPP-DCA showed less efficiency in reducing both cellular lactate levels and in the media (Figure 4). Lactate levels in the less glycolytic LNCaP cells were significantly lower than those observed in PC3 cells. Pronounced lactate concentration differences were observed between healthy glycolytic PC3 and healthy MSC cells (Figure S19B in the Supporting Information). The extent of relative decrease in glycolytic activity after treatment with Mito-DCA was similar in PC3 and LNCaP cells, and the reduction was much more significant compared to cells treated with TPP-DCA or Na-DCA (Figure S19B in the Supporting Information). None of the DCA compounds showed any effect on the lactate levels of MSC cells (Figure S19B in the Supporting Information). These observations suggested that Mito-DCA is efficient in inhibiting glycolysis only in cancer cells.

A decrease in cancer cell lactate levels is expected to be associated with an increase in ATP production. We next measured the intracellular ATP levels in PC3, LNCaP, and MSC cells treated with Mito-DCA (20 μ M), TPP-DCA (60

μ M), and Na-DCA (60 μ M). After 3 h treatment with Mito-DCA, an increase in the intracellular ATP levels was observed in PC3 cells (Figure 4). Treatment with TPP-Tris-(OH)₃ or Na-DCA did not show any significant increase in the intracellular ATP levels. TPP-DCA at three times higher concentrations showed less enhancement in intracellular ATP levels compared to Mito-DCA. Similar trends were observed in LNCaP cells upon treatment with Mito-DCA, TPP-DCA, and Na-DCA (Figure S19C in the Supporting Information). In contrast, normal MSC cells showed relatively high levels of ATP and upon treatment with all the three DCA compounds, there was marginal increase in the ATP levels (Figure S19C in the Supporting Information). At high concentrations of the DCA compounds (Mito-DCA: 50 μ M; TPP-DCA; 150 μ M; and Na-DCA: 150 μ M) with longer incubation time of 6 h, PC3 cells showed ATP reduction and cell growth inhibition (Figure S20 in the Supporting Information).

Effects of Mito-DCA on Mitochondrial Bioenergetic Functions in PC3 Cells. The selective ability of Mito-DCA in reducing lactate levels and early increase in intracellular ATP

(A) Immune response from different constructs treated PC3 cell supernatants



(B) Immune response from BMDCs activated with tumor antigens generated from PC3 cells treated with different constructs

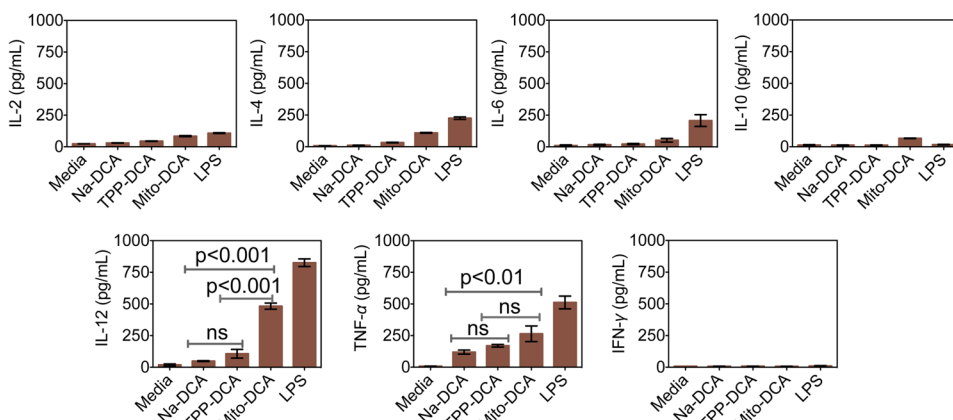


Figure 6. Lactate reduction by Mito-DCA stimulates antitumor immunity. (A) Cytokine production by PC3 cells on treatment with Mito-DCA, TPP-DCA, and Na-DCA for 24 h. (B) BMDCs activated with supernatants from PC3 cells treated with Mito-DCA, TPP-DCA, and Na-DCA show different cytokine secretion profile from the cancer cell supernatants. All data are expressed as mean \pm SD (standard deviation). A one-way ANOVA with a post-hoc Tukey test was used to identify significant differences among the groups. ns: non significant.

levels in cancer cells suggested that Mito-DCA has the potential in selectively altering the metabolism in cancer cells. To investigate this unique property of Mito-DCA in detail, we studied mitochondrial bioenergetics in PC3 cells using XF24 extracellular flux analyzer (Figure 5). We examined the metabolic fluxes of both glycolysis and OXPHOS in PC3 cells. PC3 cells were treated with Mito-DCA (10 μ M), TPP-DCA (30 μ M), and Na-DCA (30 μ M) for 4 h followed by washout and returned to fresh medium. As measures of glycolytic parameters, the changes in the extracellular acidification rate (ECAR) were monitored in response to the sequential administration of D-glucose, oligomycin, and 2-deoxy-D-glucose (2-DG) to assess glycolysis, maximal glycolytic capacity, and glycolytic reserve capacity, respectively (Figure 5A). Immediately after injecting 10 mM glucose to the treated PC3 cells in a glucose-free medium, we observed an increase in the ECAR of control, Na-DCA, and TPP-DCA treated cells. In contrast, Mito-DCA treated cells did not show any increase in the ECAR (Figure 5A). An inhibitor of mitochondrial ATP synthase, oligomycin, triggered a further change in lactic acid production as evident from ECAR levels in control, TPP-DCA, and Na-DCA treated cells, but no change was observed in Mito-DCA treated cells. Reduction of glycolysis flux by

injecting the hexokinase inhibitor 2-DG into PC3 cells induced a rapid decline in the ECAR of control cells and those treated with either TPP-DCA or Na-DCA; however, Mito-DCA treated cells did not show any significant changes. These data documented greater inhibition of glycolysis and energetic collapse in PC3 cells treated with Mito-DCA.

We next investigated basal respiration, coupling efficiency, and spare respiratory capacity in response to DCA compounds using a XF24 mito stress assay kit (Figure 5B and C). To determine whether the above-described lost glycolysis in the presence of Mito-DCA in cancer cells also affected mitochondrial respiration, we measured oxygen consumption rates (OCRs) in PC3 cells as a way of assessing OXPHOS. The basal OCR levels of PC3 cells treated with 10 μ M Mito-DCA for 3 h did not show any significant changes (Figure 5B). When the incubation period was extended to 6 h, the basal OCR levels were less than control in these cells, indicating a loss in total mitochondrial mass (Figure 5B). To capture the window where appropriate Mito-DCA concentration and suitable incubation period will show metabolic switching from glycolysis to glucose oxidation, we treated PC3 cells with 20 μ M Mito-DCA for 3 h. Under these conditions, an increase in basal OCR levels was observed indicating that the cells are using glucose

oxidation and consuming more oxygen (Figure 5B). Subsequent addition of oligomycin showed that the levels of ATP-linked respiration were attenuated in control cells or cells treated with Mito-DCA. To determine the maximal respiratory capacity, the mitochondrial uncoupler FCCP was injected into the media. The stimulation of mitochondrial respiration with FCCP after oligomycin was substantially greater in the presence of 20 μM Mito-DCA compared to the control. Injection of a combination of mitochondrial complex III inhibitor antimycin A and the mitochondrial complex I inhibitor rotenone significantly inhibited respiration in both Mito-DCA treated and control cells (Figure 5B). A comparative study of effects of Mito-DCA (10 μM , 4 h), TPP-DCA (30 μM , 4 h), and Na-DCA (30 μM , 4 h) on the OCR levels of PC3 cells showed that the OCR of Mito-DCA treated cells was less than cells treated with TPP-DCA or Na-DCA (Figure 5C). This metabolic programming of cancer cells by Mito-DCA accompanied by reduction of glycolytic activity, increase in OXPHOS, and finally overall mitochondrial mass loss indicated that mitochondria are the primary target of Mito-DCA.

Cancer Cell Lactate Reduction by Mito-DCA Results in Antitumor Immunity. Cancer cells recruit multiple pathways to evade elimination by the immune system.³² DCs, the major players for the initiation of a specific antitumor T-cell response, are the potential target for tumor-mediated immunosuppression.^{33–35} Lactic acid secretion in highly proliferative glycolytic tumors induces alteration in antigen phenotype and functional activity of DCs, which contributes to the suppression of local immunity.¹⁸ After observing significant and selective lactate reduction in PCa cells by Mito-DCA, we investigated the impact of the reduced lactate producing PC3 cell antigens on DCs. Cancer cell supernatants were generated by treating PC3 cells with Mito-DCA (50 μM), Na-DCA (150 μM), and TPP-DCA (150 μM) for 24 h. First, we looked at the immune responses from the PC3 supernatants upon treatment with different DCA compounds by determining pro-inflammatory and anti-inflammatory cytokines interleukin (IL)-2, IL-4, IL-6, IL-10, IL-12, tumor necrosis factor- α (TNF- α), and interferon- γ (IFN- γ) using enzyme-linked immunosorbent assay (ELISA) (Figure 6A).³⁶ Treatment of PC3 cells with DCA compounds resulted in up-regulation of IL-6, IL-10, and TNF- α . The levels of all these three cytokines were higher for Mito-DCA treated cells compared to those treated with TPP-DCA or Na-DCA. When DCs are activated appropriately, they take up tumor antigens and apoptotic bodies and initiate a series of actions for the selection of antigen-specific T cells and the release of cytokines such as IFN- γ and IL-12. We therefore added the PC3 supernatants containing the tumor antigens to mouse bone marrow derived DCs (BMDCs), and activation was studied using ELISA.³⁶ We observed that the BMDCs activated with cancer cell antigens generated from Mito-DCA showed significantly increased secretion of IL-12 (Figure 6B). TPP-DCA mediated increase in IL-12 from BMDCs was lesser compared to Mito-DCA. Supernatants generated from Na-DCA treatment did not show any increase in IL-12 levels. An enhanced IL-12 secretion by Mito-DCA treated tumor supernatant increases the potential of enhancing natural killer cell and cytotoxic T lymphocyte activities. Acidification by lactic acid results in the suppression of TNF- α secretion by human monocytes and mouse macrophage.³⁷ Our data showed that the cancer cell supernatant generated from the DCA compounds treatment stimulated BMDCs to secret TNF- α , and the highest level of this cytokine was observed from the supernatant that

was generated from Mito-DCA due to efficient glycolysis inhibition. These results support that Mito-DCA would be a better agent for improvement of antitumor immunity compared to the parent drug DCA.

Conclusion. In summary, the ability of Mito-DCA to alter metabolism of PCa cells suggested enormous potential and warrants further investigation. TPP-based ligands represent an important class of nonpeptidic mitochondrial targeting agents; however, prior to this work this approach was never used for DCA intracellular compartmentalization. The molecular scaffold used in Mito-DCA provides opportunities to incorporate more copies of DCA keeping a single TPP targeting moiety. The lack of sensitivity of noncancerous MSC cells to the pharmacologically relevant concentrations of Mito-DCA and three-orders of enhanced potency compared to DCA in cancer cells suggested that Mito-DCA has the potential to be nontoxic in normal tissue and highly efficacious in cancer cells. Mito-DCA showed reduced glycolytic functions, reduced basal cellular respiration, suppressed the calculated ATP synthesis, and attenuated the spare respiratory capacity in PCa cells. The effect of Mito-DCA treatments on glycolysis flux reflected its ability to reduce lactic acid production in cancer cells and simultaneously inhibit both OXPHOS and glycolysis. Effective lactate reduction in tumor cells by precise targeting of DCA to the mitochondria of cells in the form of Mito-DCA not only can change the tumor cell glycolysis efficiently but also has the potential to alter the immunosuppressive environment modulated by lactic acid. These data suggest that targeting DCA to the mitochondria can stimulate cancer cell metabolism in unique ways, which can create new strategies for DCA therapy.

METHODS

Materials and Instrumentations. A detailed description of materials and instruments is available in the Supporting Information.

Animals. Animals were obtained from Jackson Laboratory and handled in accordance with "The Guide for the Care and Use of Laboratory Animals" of the American Association for Accreditation of Laboratory Animal Care (AAALAC), Animal Welfare Act (AWA), and other applicable federal and state guidelines. All animal work presented here was approved by Institutional Animal Care and Use Committee (IACUC) of University of Georgia.

Cell Line and Cell Culture. Human PCa LNCaP, PC3, and DU145 cells were procured from the American type culture collection (ATCC). Human bone marrow derived MSCs were purchased from Lonza. DU145 cells were grown at 37 °C in 5% CO₂ in Eagle's minimum essential medium (EMEM) supplemented with 10% fetal bovine serum (FBS) and 1% penicillin/streptomycin. LNCaP and PC3 cells were grown in Roswell Park Memorial Institute (RPMI) 1640 medium. Human MSCs were grown in mesenchymal stem cell basal medium supplemented with 2% FBS, 1% penicillin/streptomycin, recombinant human fibroblast growth factor-basic (5 ng/mL), recombinant human fibroblast growth factor-acidic (5 ng/mL), and recombinant human epithelial growth factor (5 ng/mL). Cells were passed every 3–4 days and restarted from frozen stocks upon reaching pass number 20 for PC3, LNCaP, DU145, and 10 for MSC.

Synthesis of TPP-(CH₂)₅-COOH. Detailed synthetic method to TPP-(CH₂)₅-COOH and its characterizations can be found in the Supporting Information and Figures S1–S2.

Synthesis of TPP-Tris-(OH)₃. Synthesis of TPP-Tris-(OH)₃ and its characterizations can be found in the Supporting Information and Figures S3–S4.

Synthesis of Mito-DCA. A solution of TPP-Tris-(OH)₃ (0.5 g, 0.9 mmol) in CH₂Cl₂ (10 mL) was prepared in a round-bottom flask equipped with nitrogen flow. DCA anhydride (2.13 g, 8.9 mmol) was added dropwise to the solution. The reaction was stirred overnight at

RT, and the completion of the reaction was confirmed by thin layer chromatography (TLC) using a mixture of CH_2Cl_2 (95%) and CH_3OH (5%). The solvent was evaporated to dryness and Mito-DCA was purified using silica gel chromatography ($\text{CH}_2\text{Cl}_2/\text{CH}_3\text{OH}$, 95:5). Yield: 35% (0.3 g). Mp: 80–85 °C. ^1H NMR (CDCl_3): 8.3 (broad s, 1H), 7.8–7.7 (m, 1SH), 6.22 (s, 3H), 4.72 (s, 6H), 3.50 (t, 2H), 2.38 (t, 2H), 1.69 (m, 6H) ppm (Figure S5 in the Supporting Information). ^{13}C NMR (CDCl_3): δ 175.2, 163.8, 135.2, 133.6, 130.6, 118.5, 64.6, 64.5, 57.9, 36.3, 29.5, 24.4, 22.8, 20.9 ppm (Figure S5 in the Supporting Information). ^{31}P NMR (CDCl_3) 24.59 ppm (Figure S5 in the Supporting Information). HRMS-ESI (*m/z*): [M – Br]⁺ calcd for $\text{C}_{34}\text{H}_{35}\text{Cl}_4\text{NO}_7\text{P}^+$ 810.0277, found, 810.0258 (Figure S6 in the Supporting Information). Single crystals suitable for X-ray analysis were grown in CH_2Cl_2 and diethyl ether mixture (Figure 1, Figure S7, Tables S1 and S2 in the Supporting Information). Purity of Mito-DCA was checked using a high-performance liquid chromatography (HPLC) study (Figure S8 in the Supporting Information).

Synthesis of TPP-(CH_2)₃-OH. Synthesis of TPP-(CH_2)₃-OH and its characterizations can be found in the Supporting Information and Figures S9–S10.

Synthesis of TPP-DCA. A solution of TPP-(CH_2)₃-OH (0.25 g, 0.623 mmol) in CH_2Cl_2 (15 mL) was prepared in a round-bottom flask equipped with nitrogen flow. DCA anhydride (0.45 g, 1.86 mmol) was added dropwise to the solution. The reaction was stirred overnight at RT, and completion of the reaction was confirmed by TLC ($\text{CH}_2\text{Cl}_2/\text{CH}_3\text{OH}$, 90:10). The solvent was evaporated to dryness to get a pasty mass, which was further purified using silica gel chromatography ($\text{CH}_2\text{Cl}_2/\text{CH}_3\text{OH}$, 90:10). Yield: 48% (0.15 g). Mp: 75–80 °C. ^1H NMR (CDCl_3): 7.68–7.89 (m, 1SH), 6.17 (s, 1H), 4.64 (broad t, 2H), 4.13 (broad t, 2H), 2.06 (broad, 2H) ppm (Figure S11 in the Supporting Information). ^{13}C NMR (CDCl_3): δ 164.27, 135.17, 133.76, 130.49, 118.27, 66.05, 64.54, 30.90, 22.16 ppm (Figure S11 in the Supporting Information). ^{31}P (CDCl_3) NMR: 25.01 ppm (Figure S11 in the Supporting Information). HRMS-ESI (*m/z*): [M – Br]⁺ calcd for $\text{C}_{23}\text{H}_{22}\text{Cl}_2\text{O}_2\text{P}^+$ 431.0729, found, 431.0687 (Figure S12 in the Supporting Information). Purity of TPP-DCA was checked by performing a HPLC study (Figure S8 in the Supporting Information).

Single-Crystal X-ray Diffraction. Detailed descriptions of X-ray diffraction data of Mito-DCA can be found in the Supporting Information. Crystal structure data for Mito-DCA can be accessed from the Cambridge Crystallographic Data Centre (CCDC; www.ccdc.cam.ac.uk) with accession number CCDC 940383.

JC1, TMRM, MTT, and Annexin V Assays. Detailed descriptions^{8,38} of these studies can be found in the Supporting Information.

Lactate Determination and ATP Quantification. Experimental details of these studies can be found in the Supporting Information.

Seahorse XF24 Bioenergetics Assays. The three key parameters of glycolytic function, glycolysis, glycolytic capacity, and glycolytic reserve, were assessed using a Seahorse XF glycolysis stress kit in PC3 cells. Different parameters of respiration, i.e., basal respiration, coupling efficiency, and spare respiratory capacity, were investigated in PC3 cells using Seahorse XF-24 cell Mito Stress Test Kit. Detailed experimental details of these bioenergetics assays can be found in the Supporting Information.

Generation of BMDCs and Antitumor Immunity Study by ELISA. Experimental details of isolation of BMDCs from 6 to 8 weeks old C57BL/6 mice and cytokine secretion from DCs upon stimulation with cancer cell antigens derived from treatment of PC3 cells with Na-DCA, TPP-DCA, and Mito-DCA can be found in the Supporting Information.

Statistics. All data were expressed as mean \pm standard deviation. Statistical analysis were performed using GraphPad Prism software v. 5.00. Comparisons between two values were performed using an unpaired Student *t* test. A one-way ANOVA with a post-hoc Tukey test was used to identify significant differences among the groups.

ASSOCIATED CONTENT

Supporting Information

Supporting Information containing additional methods, figures, and tables. This material is available free of charge via the Internet at <http://pubs.acs.org>.

AUTHOR INFORMATION

Corresponding Author

*E-mail: shanta@uga.edu.

Author Contributions

[§]These authors contributed equally to this work.

Notes

The authors declare no competing financial interest.

ACKNOWLEDGMENTS

This work was supported by a start-up grant from the National Institutes of Health (P30GM092378) and Department of Defense Prostate Cancer Idea award (W81XWH-12-1-0406) to S.D. and a grant from the National Institutes of Health (NIH AI056484) to D.A.H. We thank S. Tundup and J. H. Choi for their help with BMDC isolation. We thank R. Tarleton for Seahorse XF analyzer and G. Cooley for assistance with XF24 analyzer. We thank N. Kolishetti for valuable comments.

REFERENCES

- (1) Warburg, O. (1956) On the origin of cancer cells. *Science* 123, 309–314.
- (2) Zu, X. L., and Guppy, M. (2004) Cancer metabolism: facts, fantasy, and fiction. *Biochem. Biophys. Res. Commun.* 313, 459–465.
- (3) Samudio, I., Fiegl, M., and Andreeff, M. (2009) Mitochondrial uncoupling and the Warburg effect: molecular basis for the reprogramming of cancer cell metabolism. *Cancer Res.* 69, 2163–2166.
- (4) Gatenby, R. A., and Gillies, R. J. (2004) Why do cancers have high aerobic glycolysis? *Nat. Rev. Cancer* 4, 891–899.
- (5) Kim, J. W., and Dang, C. V. (2006) Cancer's molecular sweet tooth and the Warburg effect. *Cancer Res.* 66, 8927–8930.
- (6) Cheong, H., Lu, C., Lindsten, T., and Thompson, C. B. (2012) Therapeutic targets in cancer cell metabolism and autophagy. *Nat. Biotechnol.* 30, 671–678.
- (7) Bonnet, S., Archer, S. L., Allalunis-Turner, J., Haromy, A., Beaulieu, C., Thompson, R., Lee, C. T., Lopaschuk, G. D., Puttagunta, L., Bonnet, S., Harry, G., Hashimoto, K., Porter, C. J., Andrade, M. A., Thebaud, B., and Michelakis, E. D. (2007) A mitochondria-K⁺ channel axis is suppressed in cancer and its normalization promotes apoptosis and inhibits cancer growth. *Cancer Cell* 11, 37–51.
- (8) Dhar, S., and Lippard, S. J. (2009) Mitaplatin, a potent fusion of cisplatin and the orphan drug dichloroacetate. *Proc. Natl. Acad. Sci. U.S.A.* 106, 22199–22204.
- (9) Sun, R. C., Fadia, M., Dahlstrom, J. E., Parish, C. R., Board, P. G., and Blackburn, A. C. (2010) Reversal of the glycolytic phenotype by dichloroacetate inhibits metastatic breast cancer cell growth in vitro and in vivo. *Breast Cancer Res. Treat.* 120, 253–260.
- (10) Pearson, H. (2007) Cancer patients opt for unapproved drug. *Nature* 446, 474–475.
- (11) Christofk, H. R., Vander Heiden, M. G., Harris, M. H., Ramanathan, A., Gerszten, R. E., Wei, R., Fleming, M. D., Schreiber, S. L., and Cantley, L. C. (2008) The M2 splice isoform of pyruvate kinase is important for cancer metabolism and tumour growth. *Nature* 452, 230–U274.
- (12) Stockwin, L. H., Yu, S. X., Borgel, S., Hancock, C., Wolfe, T. L., Phillips, L. R., Hollingshead, M. G., and Newton, D. L. (2010) Sodium dichloroacetate selectively targets cells with defects in the mitochondrial ETC. *Int. J. Cancer* 127, 2510–2519.
- (13) Jackson, V. N., and Halestrap, A. P. (1996) The kinetics, substrate, and inhibitor specificity of the monocarboxylate (lactate) transporter of rat liver cells determined using the fluorescent

- intracellular pH indicator, 2',7'-bis(carboxyethyl)-5(6)-carboxyfluorescein. *J. Biol. Chem.* 271, 861–868.
- (14) Coady, M. J., Chang, M. H., Charron, F. M., Plata, C., Wallendorff, B., Sah, J. F., Markowitz, S. D., Romero, M. F., and Lapointe, J. Y. (2004) The human tumour suppressor gene SLC5A8 expresses a Na⁺-monocarboxylate cotransporter. *J. Physiol.* 557, 719–731.
- (15) Miyauchi, S., Gopal, E., Fei, Y. J., and Ganapathy, V. (2004) Functional identification of SLC5A8, a tumor suppressor down-regulated in colon cancer, as a Na⁽⁺⁾-coupled transporter for short-chain fatty acids. *J. Biol. Chem.* 279, 13293–13296.
- (16) Li, H., Myeroff, L., Smiraglia, D., Romero, M. F., Pretlow, T. P., Kasturi, L., Lutterbaugh, J., Rerko, R. M., Casey, G., Issa, J. P., Willis, J., Willson, J. K., Plass, C., and Markowitz, S. D. (2003) SLC5A8, a sodium transporter, is a tumor suppressor gene silenced by methylation in human colon aberrant crypt foci and cancers. *Proc. Natl. Acad. Sci. U.S.A.* 100, 8412–8417.
- (17) Babu, E., Ramachandran, S., CoothanKandaswamy, V., Elangovan, S., Prasad, P. D., Ganapathy, V., and Thangaraju, M. (2011) Role of SLC5A8, a plasma membrane transporter and a tumor suppressor, in the antitumor activity of dichloroacetate. *Oncogene* 30, 4026–4037.
- (18) Gottfried, E., Kunz-Schughart, L. A., Ebner, S., Mueller-Klieser, W., Hoves, S., Andreesen, R., Mackensen, A., and Kreutz, M. (2006) Tumor-derived lactic acid modulates dendritic cell activation and antigen expression. *Blood* 107, 2013–2021.
- (19) Boddapati, S. V., D'Souza, G. G. M., Erdogan, S., Torchilin, V. P., and Weissig, V. (2008) Organelle-targeted nanocarriers: Specific delivery of liposomal ceramide to mitochondria enhances its cytotoxicity in vitro and in vivo. *Nano Lett.* 8, 2559–2563.
- (20) Smith, R. A., Porteous, C. M., Gane, A. M., and Murphy, M. P. (2003) Delivery of bioactive molecules to mitochondria in vivo. *Proc. Natl. Acad. Sci. U.S.A.* 100, 5407–5412.
- (21) Ross, M. F., Prime, T. A., Abakumova, I., James, A. M., Porteous, C. M., Smith, R. A., and Murphy, M. P. (2008) Rapid and extensive uptake and activation of hydrophobic triphenylphosphonium cations within cells. *Biochem. J.* 411, 633–645.
- (22) Marrache, S., and Dhar, S. (2012) Engineering of blended nanoparticle platform for delivery of mitochondria-acting therapeutics. *Proc. Natl. Acad. Sci. U.S.A.* 109, 16288–16293.
- (23) Marrache, S., and Dhar, S. (2013) Biodegradable synthetic high-density lipoprotein nanoparticles for atherosclerosis. *Proc. Natl. Acad. Sci. U.S.A.* 110, 9445–9450.
- (24) Marrache, S., Tundup, S., Harn, D. A., and Dhar, S. (2013) Ex vivo programming of dendritic cells by mitochondria-targeted nanoparticles to produce interferon-gamma for cancer immunotherapy. *ACS Nano* 7, 7392–7402.
- (25) Kato, M., Li, J., Chuang, J. L., and Chuang, D. T. (2007) Distinct structural mechanisms for inhibition of pyruvate dehydrogenase kinase isoforms by AZD7545, dichloroacetate, and radicicol. *Structure* 15, 992–1004.
- (26) Dhar, S., Kodama, T., and Greenberg, M. M. (2007) Selective detection and quantification of oxidized abasic lesions in DNA. *J. Am. Chem. Soc.* 129, 8702–8703.
- (27) Murphy, M. P. (2004) Investigating mitochondrial radical production using targeted probes. *Biochem. Soc. Trans.* 32, 1011–1014.
- (28) Horton, K. L., Pereira, M. P., Stewart, K. M., Fonseca, S. B., and Kelley, S. O. (2012) Tuning the activity of mitochondria-penetrating peptides for delivery or disruption. *ChemBioChem* 13, 476–485.
- (29) Benedettini, E., Nguyen, P., and Loda, M. (2008) The pathogenesis of prostate cancer: from molecular to metabolic alterations. *Diagn. Histopathol.* 14, 195–201.
- (30) Higgins, L. H., Withers, H. G., Garbens, A., Love, H. D., Magnoni, L., Hayward, S. W., and Moyes, C. D. (2009) Hypoxia and the metabolic phenotype of prostate cancer cells. *Biochim. Biophys. Acta* 1787, 1433–1443.
- (31) Helman, L. J., and Meltzer, P. (2003) Mechanisms of sarcoma development. *Nat. Rev. Cancer* 3, 685–694.
- (32) Kim, R., Emi, M., and Tanabe, K. (2007) Cancer immunoediting from immune surveillance to immune escape. *Immunology* 121, 1–14.
- (33) Gabrilovich, D. I., Chen, H. L., Girgis, K. R., Cunningham, H. T., Meny, G. M., Nadaf, S., Kavanaugh, D., and Carbone, D. P. (1996) Production of vascular endothelial growth factor by human tumors inhibits the functional maturation of dendritic cells. *Nat. Med.* 2, 1096–1103.
- (34) Radmayr, C., Bock, G., Hobisch, A., Klocker, H., Bartsch, G., and Thurnher, M. (1995) Dendritic antigen-presenting cells from the peripheral blood of renal-cell-carcinoma patients. *Int. J. Cancer* 63, 627–632.
- (35) Orsini, E., Guarini, A., Chiaretti, S., Mauro, F. R., and Foa, R. (2003) The circulating dendritic cell compartment in patients with chronic lymphocytic leukemia is severely defective and unable to stimulate an effective T-cell response. *Cancer Res.* 63, 4497–4506.
- (36) Marrache, S., Choi, J. H., Tundup, S., Zaver, D., Harn, D. A., and Dhar, S. (2013) Immune stimulating photoactive hybrid nanoparticles for metastatic breast cancer. *Integr. Biol.* 5, 215–223.
- (37) Dietl, K., Renner, K., Dettmer, K., Timischl, B., Eberhart, K., Dorn, C., Hellerbrand, C., Kastenberger, M., Kunz-Schughart, L. A., Oefner, P. J., Andreesen, R., Gottfried, E., and Kreutz, M. P. (2010) Lactic acid and acidification inhibit TNF secretion and glycolysis of human monocytes. *J. Immunol.* 184, 1200–1209.
- (38) Pathak, R. K., Marrache, S., Choi, J. H., Berding, T. B., and Dhar, S. (2014) The prodrug Platin-A: simultaneous release of cisplatin and aspirin. *Angew. Chem., Int. Ed.* 53, 1963–1967.